Annealing of Linear Birefringence in Single-Mode Fiber Coils: Application to Optical Fiber Current Sensors

Dingding Tang, A. H. Rose, G. W. Day, and Shelley M. Etzel

Abstract—**Annealing procedures that greatly reduce linear birefringence in single-mode fiber coils are described in detail. These procedures have been successfully applied to coils ranging from 5 mm to 10 cm in diameter and up to 200 or more turns. They involve temperature cycles that last 3–4 days and reach maximum temperatures of about 850°C. The residual birefringence and induced loss are minimized by proper selection of fiber. The primary application of these coils is optical fiber current sensors, where they yield small sensors that are more stable than those achieved by other techniques. A current sensor with a temperature stability of $+8.4 \times 10^{-5}$/K over the range from −75 to +145°C has been demonstrated. This is approximately 20% greater than the temperature dependence of the Verdet constant. Packaging degrades the stability, but a packaged sensor coil with a temperature stability of about $+1.6 \times 10^{-4}$/K over the range from −20 to +120°C has also been demonstrated.**

I. Introduction

ALTHOUGH single-mode fibers with very low inherent linear birefringence [1] are now readily available, there remains the problem that when these fibers are formed into the proper configuration for many sensing applications, significant linear birefringence is induced by bending. This bend-induced birefringence is the primary difficulty in the development of optical fiber current sensors based on the Faraday effect [2]–[4].

Bending of a single-mode optical fiber induces a phase retardation (retardance per unit length) of [5]

$$\Delta\beta = \frac{\pi}{\lambda} EC \frac{r^2}{R^2} \text{ rad/m}, \tag{1}$$

where E is Young's modulus, C is the stress-optic coefficient, r is the radius of the fiber, R is the radius of the bend, and λ is the operating wavelength. For silica, $E = 7.45 \times 10^9$ Pa [6] and $C = -3.34 \times 10^{-11}$ Pa^{-1} at $\lambda = 633$ nm [7].

Manuscript received December 6, 1990. This work has been supported in part by NASA through the Lewis Research Center, the Department of Defense through the Defense Nuclear Agency and the Department of the Navy, and the Department of Energy through the Los Alamos National Laboratory.

The authors are with the National Institute of Standards and Technology, Boulder, CO 80303.

IEEE Log Number 9100463.

For current sensors, it is more useful to consider the retardation per turn, which is given by

$$\Delta\beta = \frac{2\pi^2}{\lambda} EC \frac{r^2}{R} \text{ rad/turn}. \tag{2}$$

Thus, for example, a 3-cm-diameter coil of 125-μm-diameter fiber has a retardation of approximately 1.6 rad/turn at a wavelength of 800 nm.

We have previously shown that fiber bend birefringence can be greatly reduced by annealing [8]. Stone [9] has shown that inherent birefringence can also be reduced by annealing. In this paper, we expand upon this previous work and focus on the annealing of coils for current sensors. We describe our procedure for annealing in greater detail that has previously been reported. We explain the importance of fiber selection in minimizing residual birefrigence and induced loss. We describe the typical temperature dependence of the residual birefrigence. And we report what we believe is the best temperature stability for a fiber current sensor yet obtained.

II. Annealing Procedure

Fiber to be annealed is wrapped around a mandrel of the desired diameter. The mandrel is removed and the coil is placed in a channel machined into a ceramic annealing fixture (Fig. 1) where it is held with several ceramic wedges. The channel is approximately 3 mm wide and 8 mm deep. We presently produce coils with nominal diameters ranging from 5 mm to 10 cm and with greater than 200 hundred turns.

To anneal the fiber we use a temperature controlled oven. The temperature is raised to about 850°C at about 5°C/min and held at the maximum temperature for about 24 h. The coil is then cooled at about 0.2°C/min until it reaches room temperature in about 3 days. We have not attempted to optimize the annealing cycle to achieve the best coil characteristics in the shortest time. Using a higher temperature might speed the process [9] as could increasing the cooling rate after the temperature falls below the strain point of the glass [10].

The coils are annealed in air. Normal buffer coatings oxidize at temperatures of 300 to 400°C, damaging the surface of the glass and resulting in a shattered coil. One

U.S. Government work not protected by U.S. copyright

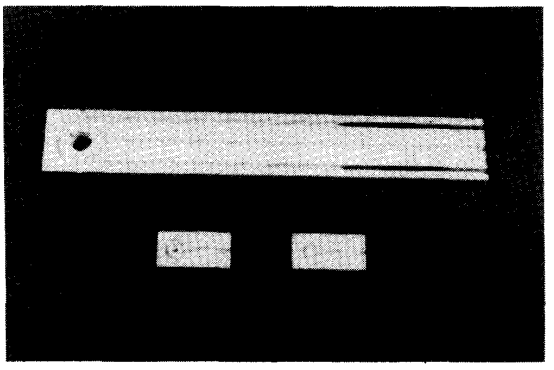

Fig. 1. Ceramic fixtures used for annealing fiber coils.

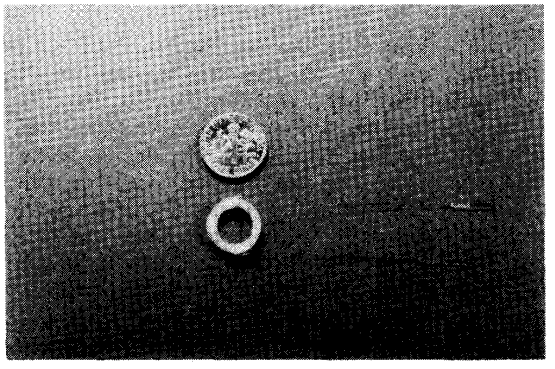

Fig. 2. A 1-cm diameter, 200 turn, annealed coil.

solution to this problem is to remove the coatings prior to annealing. This can be done successfully for relatively large coils with a small numbers of turns, but often results in broken coils. We have found, however, that if the coated fibers are pretreated by soaking in a solvent, typically acetone or methylene chloride, depending on the coating used, oxidation will occur with minimal effect on the strength of the fiber. The solvent loosens the fiber coating from the glass and probably speeds its oxidation.

When cool, the coils are removed from the oven and from the annealing fixture. They then retain their coiled configuration without constraint (Fig. 2) and can withstand limited handling. They must be protected, however, before they can be extensively tested or used. For this purpose, we use a plastic package, generally either polycarbonate or phenolic, which has a channel similar to that in the annealing fixture (Fig. 3) machined into it. The coil is surrounded in the package by a very viscous lubricant that can be used over a broad temperature range. The coils are generally tested both in the annealing fixture and the plastic package.

III. Selection of Fiber

The properties of the annealed coil, specifically its optical attenuation, cutoff wavelength, and polarization properties depend substantially on the type of fiber used.

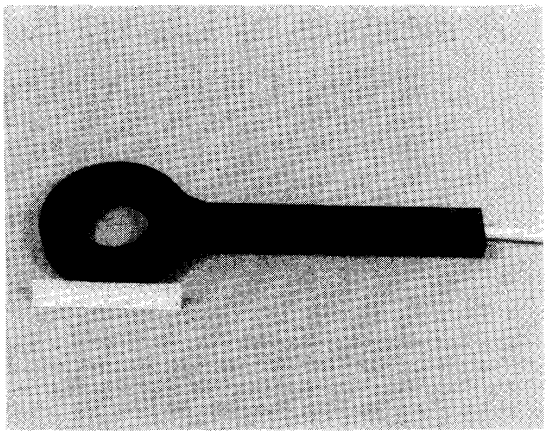

Fig. 3. A packaged coil. Coil diameter is approximately 5 cm. The package is 30 cm long.

We have investigated the suitability of a number of fibers for these applications. Most were ordinary, 125-μm diameter, telecommunications fiber, though usually with cutoff wavelengths in the 600–900-nm range. We select fibers for relatively low inherent birefringence, and generally choose fiber with an inherent retardation of the order of 50°/m or less. We have also experimented with specialty fibers, including "spun fibers" [1] and, for very small coils, 80-μm-diameter fiber. The choice of dopants is also important, as indicated below.

A. Minimizing Residual Loss

In some fibers, annealing induces significant changes in the spectral attenuation and cutoff wavelength of the fiber. In part, this results from the fact that the refractive index of silica containing certain dopants, especially boron, depends on its thermal history [11], [12]. Other, not yet understood, mechanisms also appear to be important.

To investigate these effects, we have made spectral attenuation measurements on coils of several different fibers, both annealed and unannealed. The measurement was similar to that commonly used for cutoff wavelength measurements [13], in which the attenuation of a length of fiber including a coil is compared to that of a straight length of fiber. To be consistent, we used 10 turn, 3-cm-diameter coils in all of these measurements. Generally, repeated testing on the same fiber gave very similar results.

Figs. 4 and 5 show the results for two germania core, silica clad fibers. These were produced by two different companies, both using outside vapor deposition. Apparently, they differ primarily in their cutoff wavelengths and numerical apertures. After annealing, both show a small shift of the cutoff wavelength to longer wavelengths. The lower NA fiber (Fig. 5) also shows a broad region of increased attenuation on the long wavelength side of cutoff. The source of this loss is as yet unexplained.

Fig. 6 shows the results for another germania core fiber, this one having a very slightly depressed inner clad-

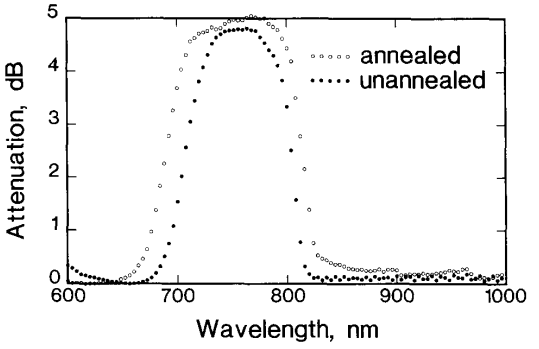

Fig. 4. Spectral attenuation of annealed and unannealed coils of a fiber with Ge : SiO_2 core and SiO_2 cladding. NA = 0.138.

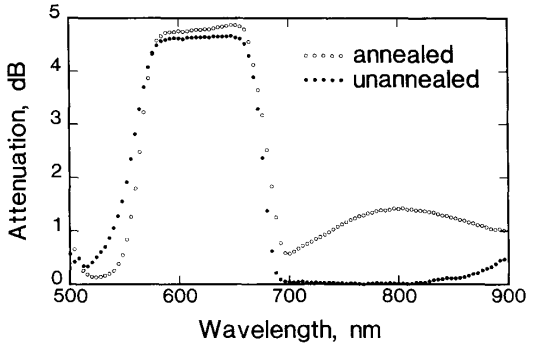

Fig. 5. Spectral attenuation of annealed and unannealed coils of a fiber with Ge : SiO_2 core and SiO_2 cladding. NA = 0.11.

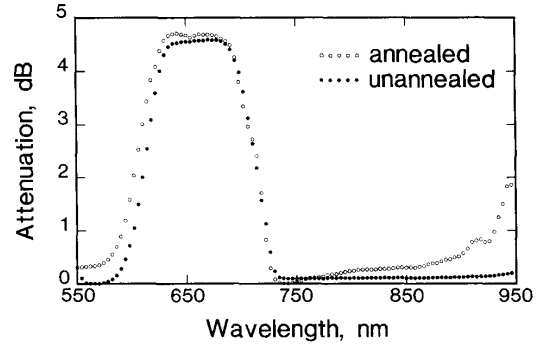

Fig. 6. Spectral attenuation of annealed and unannealed coils of a fiber with Ge : SiO_2 core, slightly depressed inner cladding doped with phosphorus and fluorine, and SiO_2 cladding. NA = 0.13.

ding incorporating phosphorus and fluorine. It was produced by MCVD technology and was spun during drawing [1] to reduce inherent birefringence. After annealing it shows essentially no shift in cutoff wavelength, but does show evidence of increased microbending loss at longer wavelengths.

Fig. 7 shows the results for a fiber with a germania core and a depressed cladding incorporating boron and a small amount of fluorine. After annealing, the cutoff wavelength of this fiber is shifted about 60 nm to shorter wavelengths, and increased loss at longer wavelengths similar to that shown in Fig. 5 is observed. The shift in cutoff wavelength is consistent with measured changes in the refractive-index profile.

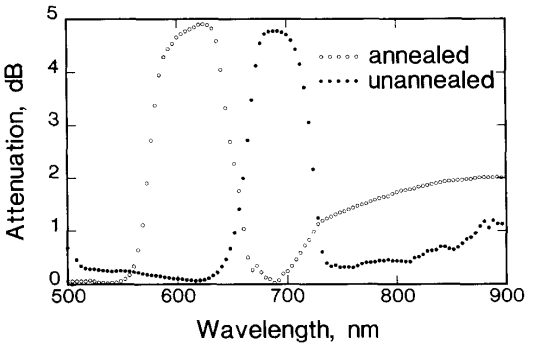

Fig. 7. Spectral attenuation of annealed and unannealed coils of a fiber with Ge : SiO_2 core and B : SiO_2 cladding. NA = 0.16.

All of the fibers represented in Figs. 4–6, and perhaps even the fiber of Fig. 7, can be used with relatively little loss, provided that the wavelength is suitably chosen. In some cases, especially for coils smaller than 3 cm, we find it best to operate at a wavelength for which the fiber supports two modes, but for which the LP_{11} mode has a high attenuation when the fiber is coiled: a wavelength of 650 nm for the fiber of Fig. 5, for example.

B. Residual Retardance

We characterize the coils after annealing as though they consist, end to end, of a single discrete linear retarder and a single discrete circular retarder (rotator) (Fig. 8) [14]. The measurements are made polarimetrically. Normally the residual birefringence is small enough that 2π ambiguities are not a problem; otherwise, a larger-than-assumed retardance is revealed when the coils are tested as current sensors.

Fig. 9 shows residual retardance versus temperature for a coil made with fiber from the same preform as that described in Fig. 4. The coil consisted of 55 turns at a 4.5-cm mean diameter. It was designed for and tested at a wavelength of 780 nm. The measurements were made after the coil was removed from the annealing fixture, but before any protective material was applied to the fiber. When straight, the fiber has a typical retardation of about 20°/m at that wavelength, or about 160° in the 8 m of fiber used in the coil. These values are based on extrapolation of measurements made at a longer wavelength. By calculation (2), the bend retardance prior to annealing was about 3500° at 780 nm. The room temperature retardance after annealing was about 65°, that is, about 1.2°/turn or 8°/m; this shows that, not only was the bend birefringence reduced substantially, but that the inherent birefringence was also reduced.

This coil shows the best temperature stability yet achieved. Above about −30°C, the slope of the retar-

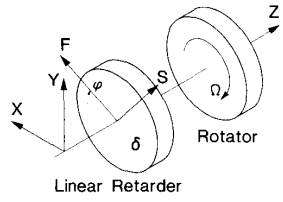

Fig. 8. Model for the birefringence of a coil consisting of two elements: a linear retarder of magnitude δ, its fast axis oriented at angle φ to an arbitrarily defined x axis, and a rotator of magnitude Ω.

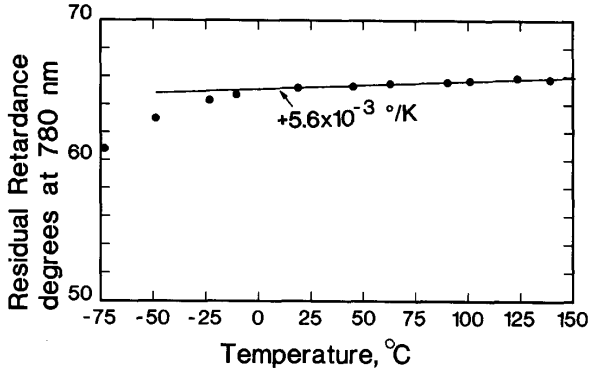

Fig. 9. Residual retardance versus temperature for a 55 turn, 4.5-cm mean diameter coil made with the fiber described in Fig. 4.

dance-versus-temperature curve is $+5.6 \times 10^{-3}$°/K. There are several possible explanations for the more rapid change in retardance at lower temperatures; no verification was attempted.

Fig. 10 shows the residual retardance versus temperature for a coil similar to that of Fig. 9, except that it had been encapsulated in a high viscosity lubricant and enclosed in a polycarbonate package. At temperatures above −30°C the retardance changes with temperature by about -2.6×10^{-2}°/K. At lower temperatures, the retardance increases rapidly, probably due to the hardening of the lubricant.

Fig. 11 shows the relative magnitude of the rotation elements for coils made with two different fibers. The "conventional" fiber was similar to that described in Fig. 4. The "spun" fiber was similar to that described in Fig. 6. Each consisted of 55 turns at a mean diameter of 4.5 cm. The coil made from " conventional fiber" shows essentially no change in rotation with temperature, and is typical of coils produced from most fibers. The coil made from "spun fiber" shows a substantial change in rotation with temperature, and seems to be typical of that type of fiber. This rotation is undesirable in most sensor configurations.

C. Summary of Fiber Considerations

Even though these experiments demonstrate that annealing reduces both bend and inherent birefringence, we generally find that fibers with lower inherent birefringence yield a lower residual birefringence. We suspect that the residual birefringence is primarily limited by geometrical imperfections in the fiber, especially noncircularity of the core.

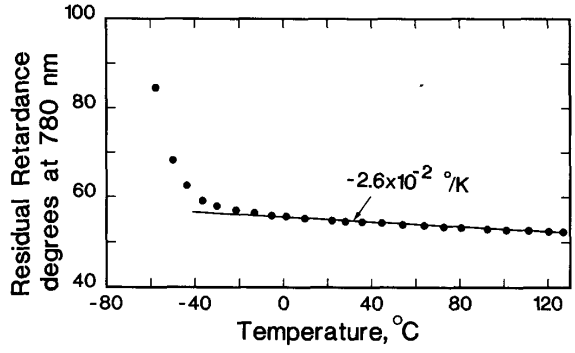

Fig. 10. Residual retardance of a coil similar to that described in Fig. 9, except that it had been encapsulated in a high viscosity lubricant and a phenolic package.

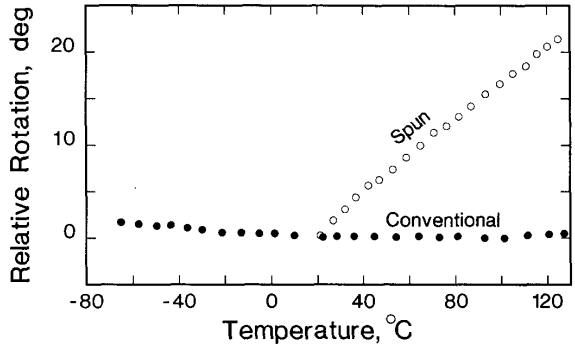

Fig. 11. Relative magnitude of the rotation elements for coils of two different fibers. Both coils were 55 turns at a mean diameter of 4.5 cm. The "conventional" fiber is the same as that of Figs. 4 and 9. The "spun" fiber is the same as that of Fig. 6.

Aside from the advantage of avoiding boron as a dopant, it is difficult to generalize about the importance of composition and index profile. The higher NA Ge:SiO_2 fibers tested here (Figs. 4 and 6) show less change in their spectral transmittance after annealing than the lower NA fiber (Fig. 5), though this many be coincidental. Careful investigation of the changes of refractive index with thermal history for other dopants could lead to index profiles that will change less during annealing. This could be important, not only for annealed coils, but also in other applications where high temperatures are encountered.

IV. Current Sensor Performance

Ideally, in a fiber current sensor the plane of polarization of linearly polarized light propagating in a fiber coil surrounding a conductor is rotated by an angle θ, given by

$$\theta = \mu VNI \tag{3}$$

where μ is the permeability of the fiber, V is a material parameter known as the Verdet constant, N is the number of turns in the coil, and I is the current flowing through the coil [3], [4]. If the light emerging from the coil passes through a polarizer oriented at an angle φ to the zero-current output plane of polarization, the transmittance as a function of current, which we call the response function, is given by

$$R(I) = \sin^2 (\mu VNI + \varphi). \tag{4}$$

For the case of $\varphi = 45°$ which is commonly used when measuring small currents, we can define the sensitivity S of the sensor as the slope of the response function at zero current $S = \mu VN$. Often two outputs with $\varphi = \pm 45°$ are used, and the ratio of the difference to their sum is obtained electronically or numerically. This doubles the sensitivity, provides a bipolar response, and reduces the effect of source drift and relative intensity noise. The resulting response function is

$$R(I) = \sin (2\mu VNI). \tag{5}$$

A. Stability

When linear birefringence is present, the response function is distorted [3], [4]. Assuming that the retardance of the coil is evenly distributed and fixed in orientation, and that the current is centered in the coil, the response function for the difference-over-sum case described in the preceding paragraph becomes, rather than (5)[1]

$$R(I) = 2\mu VNI \left(\frac{\sin \sqrt{\delta^2 + (2\mu VNI)^2}}{\sqrt{\delta^2 + (2\mu VNI)^2}} \right) \tag{6}$$

where δ is the retardance of the coil. Equation (6) reduces to (5) when δ is small. It also reduces to (5) when the Faraday rotation ($2\mu VNI$) is significantly larger than the linear retardance (δ); in other words, the distortion of the response function occurs primarily for small currents. From (6) we obtain the small-current sensitivity as a function of retardance

$$S = \left. \frac{dR(I)}{dI} \right|_{I=0} = 2\mu VN \frac{\sin \delta}{\delta}. \tag{7}$$

The temperature dependence of the sensitivity is then

$$\frac{1}{S}\frac{dS}{dT} = \frac{1}{V}\frac{dV}{dT} + \left(\cot \delta - \frac{1}{\delta} \right) \frac{d\delta}{dT} \tag{8}$$

or for small δ

$$\frac{1}{S}\frac{dS}{dT} \approx \frac{1}{V}\frac{dV}{dT} - \frac{\delta}{3}\frac{d\delta}{dT}. \tag{9}$$

[1] Equation (6) can be derived using Jones calculus and the Jones matrix for a medium having both linear and circular birefringence. The method is illustrated, for example, in A. M. Smith, "Polarization and magnetooptic properties of single-mode fiber," *Appl. Opt.*, vol. 17, pp. 52–56, 1978.

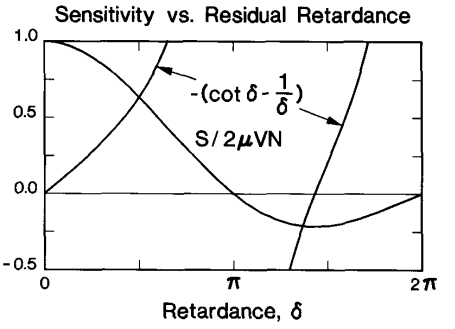

Fig. 12. The normalized sensitivity of a current sensor as a function of residual retardance δ is $(\sin \delta)/\delta$ (7). Its partial derivative with respect to retardance is $(\cot \delta - 1/\delta)$ (8).

The first term on the right side of (8), the temperature dependence of the Verdet constant, has recently been measured for several diamagnetic glasses [15]. For SiO_2, $(dV/dT)/V$ is $+6.9 \times 10^{-5}$/K. The quantity $(\cot \delta - 1/\delta)$ in the second term, which is the normalized derivative of $(\sin \delta)/\delta$, is plotted in Fig. 12, along with $(\sin \delta)/\delta$. The third quantity in (8), the temperature derivative of the retardance, $d\delta/dT$, is found experimentally to take either sign.

The sensitivity is obviously greatest when the retardance is small. If this is the case and if the magnitude of the residual retardance decreases with temperature, the retardance term in (8) is positive, and $(dV/dT)/V$ is the best stability that can be obtained. If, on the other hand, the magnitude of the residual retardance increases with temperature, the second term is negative and compensation can occur.

Rogers [4] has pointed out that there are other stable conditions where $\cot \delta - 1/\delta = 0$. The first occurs at $\delta = 4.5$ rad. Operation at this point would be accompanied by a loss in sensitivity of more than a factor of 4 and a phase reversal. Compensation could also occur in this case. Subsequent points of stability probably are accompanied by too great a loss of sensitivity to be useful.

Another problem arises when the inherent rotation of the coil, that is the zero-current output plane of polarization, is unstable, as is the case with "spun" fiber in Fig. 11. This is equivalent to a change in φ (4), that is, a shift in the response function that would make dc measurements impossible and, if large enough, degrade ac measurements as well. However, since this rotation is reciprocal, it should be possible to compensate for it by using a two-pass configuration, reflecting the light from the far end of the coil.

B. Experimental Results

We typically measure the low frequency sensitivity of a current sensor with a 100-Hz ac current of about 500 mA in a single conductor through the coil. The detected signals are monitored with a lockin amplifier or a spectrum analyzer. Measurements are made as a function of

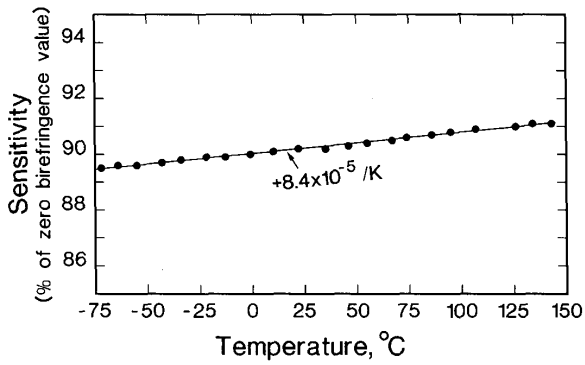

Fig. 13. Sensitivity versus temperature data for the unpackaged coil of Fig. 9.

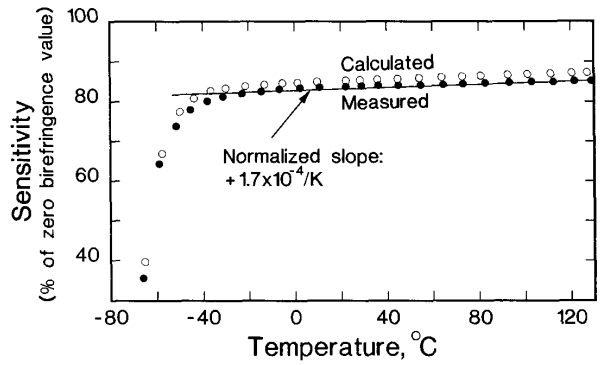

Fig. 14. Sensitivity versus temperature for the packaged coil of Fig. 10.

temperature, point by point, in an environmental chamber.

Fig. 13 shows the sensitivity versus temperature for the unpackaged coil for which the retardance versus temperature data are presented in Fig. 9. The slope of the line is $+8.4 \times 10^{-5}$/K, or about 20% greater than the temperature dependence of the Verdet constant.

However, since the residual retardance increased with temperature in this case, we expected partial compensation to occur and the total temperature dependence of the sensitivity to be smaller than that of the Verdet constant alone. Specifically, (8) yields a projected temperature dependence of $+2.8 \times 10^{-5}$/K. There are several potential explanations for not observing compensation; these relate to the location of the retardance in the coil and leads, and have yet to be explored. In any case, the result of Fig. 13 demonstrates the feasibility of a current sensor with a temperature stability approaching the material limit.

Fig. 14 shows the current sensitivity versus temperature for the packaged coil described above and in Fig. 10. At temperatures above -30°C the sensitivity increases by $+1.7 \times 10^{-4}$/K. These data are more consistent with the measured retardance data than those for the unpackaged coil. The predicted sensitivity versus temperature, calculated using (8) and measured retardance data, is also shown in Fig. 14. Above -30°C the predicted slope is $+2.3 \times 10^{-4}$/K, or about 35% greater than that measured. The sharp decrease in sensitivity at temperatures below -30°C is consistent with the increase in birefringence at those temperatures.

V. Comparison to Other Approaches

The use of annealed coils for current sensors should be compared to other approaches for reducing the problems caused by linear birefringence in the fiber.

The earliest and simplest approach is the use of twisted fiber [2]. Twisting adds circular birefringence to the fiber, in essence biasing or shifting the distorted part of the response function (6) away from the origin. It is effective for relatively large coils with few turns. For small coils, the twist necessary to achieve a useful effect often exceeds the breaking strength of the fiber. Further, the twist-induced circular birefringence is temperature dependent, thereby introducing a stability problem. Nonetheless, primarily because of its simplicity, the use of twisted fiber remains attractive in sensors where long-term stability is not important, for example, in the measurement of large pulsed currents.

A second approach is the use of a fiber with a high circular birefringence. Circular birefringence causes a rotation of the plane of polarization that merely adds to that caused by the Faraday effect. If the circular birefringence is sufficiently large, linear birefringence arising from bending or other effects has little effect (6). Truly circularly birefringent fibers have been demonstrated [16], but suffer from practical difficulties. An alternative is an elliptically birefringent fiber produced by spinning a preform with high linear birefringence while it is pulled into fiber [17]. The Faraday effect in such a fiber is reduced according to the extent to which the eigenmodes are elliptical rather than circular. Good sensitivity (98% of theoretical) has been achieved in sensors with a diameter of 12 mm [18], and sensors as small as 7 mm in diameter have been demonstrated [17]. These sensors have excellent immunity to mechanical perturbations. A further advance is that a coil of such fiber can be wrapped around a conductor without breaking the electrical path. The large temperature dependence of the elliptical birefringence remains a problem. That difficulty can be addressed by using a spectrally broad source and a two-pass optical configuration; with these techniques a temperature stability of $+5 \times 10^{-4}$/K, has been demonstrated [18].

Current sensors based on annealed coils offer better temperature stability than has been achieved with either of the other approaches, with the additional possibility, in principle, of reducing the temperature dependence below that of the Verdet constant. A further advantage is that annealed coils can be inexpensively produced from ordinary telecommunications fiber. The principal difficulty is that the coils must be carefully packaged for protection and to minimize sensitivity to vibration.

ACKNOWLEDGMENT

The authors would like to thank M. Young for measuring the fiber index profiles.

REFERENCES

[1] D. N. Payne, A. J. Barlow, and J. J. Ramskov Hansen, "Development of low- and high-birefringence optical fibers," *IEEE J. Quantum Electron.*, vol. QE-18, pp. 477–488, 1982.
[2] S. C. Rashleigh and R. Ulrich, "Magneto-optic current sensing with birefringent fibers," *Appl. Phys. Lett.*, vol. 34, pp. 768–770, 1979.
[3] G. W. Day and A. H. Rose, "Faraday effect sensors: The state of art," in *Proc. SPIE*, vol. 985, pp. 138–150, 1988.
[4] A. J. Rogers, "Optical-fibre current measurement," *Int. J. Optoelectronics*, vol. 3, pp. 391–407, 1988.
[5] R. Ulrich, S. C. Rashleigh, and W. Eickhoff, "Bending-induced birefringence in single-mode fibers," *Opt. Lett.*, vol. 5, pp. 273–275, 1980.
[6] N. F. Borrelli and R. A. Miller, "Determination of the individual strain-optic coefficients of glass by ultrasonic technique," *Appl. Opt.*, vol. 7, pp. 748–750, 1968.
[7] Y. Namihira, "Opto-elastic constant in single-mode optical fibers," *J. Lightwave Technol.*, vol. LT-3, pp. 1078–1083, 1983.
[8] G. W. Day and S. M. Etzel, "Annealing of bend-induced birefringence in fiber current sensors," in *Tech. Dig. IOOC/ECOC '85* (Venice, Italy), 1985, pp. 871–874.
[9] J. Stone, "Stress-optic effects, birefringence, and reduction of birefringence by annealing in fiber Fabry-Perot interferometers," *J. Lightwave Technol.*, vol. 6, pp. 1245–1248, 1988.
[10] C. L. Babcock, *Silicate Gate Technology Methods*. New York: Wiley, 1977.
[11] I. Fanderlik, *Optical Properties of Glass (Glass Science and Technology 5)*. Amsterdam: Elsevier, 1983, ch. 4.
[12] W. T. Anderson, P. F. Glodis, D. L. Philen, A. A. Schenk, and C. L. Bice, "Thermally induced refractive-index changes in a single-mode optical-fiber preform," in *Tech. Dig. OFC'84*, 1984, pp. 78–79.
[13] D. L. Franzen, "Determining the effective cutoff wavelength of single-mode fibers: An interlaboratory comparison," *J. Lightwave Technol.*, vol. LT-3, pp. 128–134, 1985.
[14] Henry Hurwitz, Jr. and R. Clark Jones, "A new calculus for the treatment of optical systems. II. Proof of three general equivalence theorems," *J. Opt. Soc. Amer.*, vol. 31, pp. 493–499, 1941.
[15] P. A. Williams, A. H. Rose, G. W. Day, T. E. Milner, and M. N. Deeter, "Temperature dependence of the verdet constant in several diamagnetic glasses," *Appl. Opt.*, vol. 30, pp. 1176–1178, 1991.
[16] M. P. Varnham, R. D. Birch, and D. N. Payne, "Helical core circularly birefringent fibres," in *Tech. Dig. IOOC/ECOC'85* (Venice, Italy), 1985, pp. 135–138.
[17] R. I. Laming, D. N. Payne, and L. Li, "Current monitor using elliptical birefringent fiber and active temperature compensation," in *Proc. SPIE*, vol. 789, pp. 283–287, 1987.
[18] R. I. Laming, D. N. Payne, "Electric current sensors employing spun highly birefringent optical fibers," *J. Lightwave Technol.*, vol. 7, pp. 2084–2094, 1989.

Dingding Tang received the B.S. degree in electronics from Tsinghua University, Beijing, China, in 1968 and the M.S. degree in applied physics from Shanghai Jiaotong University, Shanghai, China, in 1981.

In 1981 he joined the Shanghai Institute of Ceramics, Chinese Academy of Sciences, as a Research Assistant Professor. There his research was concerned with the fabrication and characterization of optical fiber, and its application to sensors and communications. Since 1987 he has been a Guest Scientist with the National Institute of Standards and Technology in Boulder, CO, where he has been engaged in research on the polarization properties of optical fiber and the development of optical fiber sensors.

*

A. H. Rose received the B.S. degree in physics at Abilene Christian University, Abilene, TX, in 1981 and the M.S. and Ph.D. degrees in physics at the University of Arkansas, Fayetteville, in 1983 and 1986, respectively. His graduate research was the development and application of photodeflection and photoacoustic spectroscopy to combustion diagnostics. He joined the U.S. Army's Ballistic Research Laboratory, Aberdeen Proving Ground, MD, as an NRC Postdoctoral Fellow in 1986.

In 1987 he joined the National Bureau of Standards (NBS), renamed the National Institute of Standards and Technology (NIST), Boulder, CO, to work on the development of optical fiber sensors that measure electric and magnetic fields.

Dr. Rose is a member of the Optical Society of America.

*

G. W. Day received the B.S., M.S., and Ph.D. degrees in electrical engineering from the University of Illinois, Urbana, in 1966, 1967, and 1970, respectively.

In 1969, he joined the National Bureau of Standards as an NBS/NRC Postdoctoral Fellow and has remained with that organization, now called the National Institute of Standards and Technology. His research has spanned a wide range of problems in the characterization of optical electronic devices and components, focusing especially on optical fiber and optical detectors. Since 1982 he has been responsible for research on optical fiber sensors, primarily for electromagnetic measurements. He has been an Adjunct Professor of Physics at the Colorado School of Mines, a Visiting Fellow at the University of Southampton, and a Visiting Lecturer in Electrical Engineering at the University of Colorado. In 1980 he helped organize the first biennial Symposium on Optical Fiber Measurements, and continues as its program chairman. He has received both the Gold and Silver Medals of U.S. Department of Commerce and an IR-100 Award from Industrial Research Magazine for his research.

*

Shelley M. Etzel received the B.A. degree in general studies from the University of Iowa, Iowa City, in 1987.

She joined the National Bureau of Standards (now the National Institute of Standards and Technology) in 1978 and has worked on laser power and energy measurements, optical fiber characterization, and optical fiber sensors.